Dowd and Paik and assigned to triplet **3**,[6] actually does belong to this diradical.

Acknowledgment. We thank the National Science Foundation for support of this research. The purchase of the Convex C-1 computer, which was used for some of the calculations, was also made possible by a grant from NSF. Several of the calculations reported here were performed at the San Diego Supercomputer Center, which we thank for a generous grant of supercomputer time.

Supplementary Material Available: UHF 6-31G* geometries and energies of the lowest triplet state of **1–3** (3 pages). Ordering information is given on any current masthead page.

Origin of Metal Clustering in Transition-Metal Chalcogenide Layers MX_2 (M = Nb, Ta, Mo, Re; X = S, Se)

Enric Canadell,*[1a] Albert LeBeuze,*[1b] Moulay Abdelaziz El Khalifa,[1b] Roger Chevrel,[1c] and Myung-Hwan Whangbo*[1d]

Contribution from the Laboratoire de Chimie Théorique,† Bât. 490, Université de Paris-Sud, 91405 Orsay, France, Laboratoire de Chimie Théorique, Université de Rennes I, 35042 Rennes, France, Laboratoire de Chimie Minérale B, Université de Rennes I, 35402 Rennes, France, and Department of Chemistry, North Carolina State University, Raleigh, North Carolina 27695-8204. *Received September 15, 1988*

Abstract: The origin of metal clustering in transition-metal layers MX_2 (M = transition metal, X = chalcogen) was examined by performing tight-binding band electronic structure calculations on $CoMo_2S_4$, V_3S_4, Mo_2S_3, and Nb_2Se_3. Since all MX_2 layers that exhibit metal clustering have double octahedral M_2X_6 chains as their building blocks, we analyzed the metal clustering in the MX_2 layers as a phenomenon concerning its building blocks, M_2X_6 chains. Our study shows that the metal clustering in an MX_2 layer of d^2 ions arises from the metal–metal bond formation across shared octahedral edges between MX_4 chains of each M_2X_6 chain. The metal clustering in an MX_2 layer of d^3 ions is a consequence of the Peierls distortion associated with the half-filled t_{2g} block bands of its building blocks, M_2X_6 chains.

Metal clustering is often observed in MX_2 layers made up of MX_6 octahedra (M = transition metal, X = halogen).[2-7] It is appealing to analyze the origin of the metal clustering from the viewpoint of the electronic structure change associated with a distortion from an ideal, hexagonal MX_2 layer.[8] However, this analysis is complicated due to the absence of simple distortion parameters connecting the ideal structure to the real one. All MX_2 layers that show metal clustering have M_2X_6 chains as their building blocks (vide infra), so it would be simple to describe the metal clustering as a phenomenon concerning the M_2X_6 chains rather than the MX_2 layers. This alternative approach provides a much simpler description for the crystal and electronic structures of numerous transition-metal chalcogenides containing MX_2 layers, which include ReX_2 (X = S, Se),[2] $M'Mo_2S_4$ (M' = V, Cr, Fe, Co),[3] NiV_2X_4 (X = S, Se),[4] V_3X_4 (X = S, Se),[5] Mo_2S_3,[6] and M_2Se_3 (M = Nb, Ta).[7] In the present work, we discuss the electronic structures of these compounds from the viewpoint of their building blocks, M_2X_6 chains. In the following, the structural patterns of those compounds are briefly reviewed, and the origin of their metal clustering is discussed in terms of the tight-binding band electronic structures calculated for several representative examples.

M_2X_6 Chains as Building Blocks

An ideal MX_4 chain **1** is obtained from regular MX_6 octahedra upon edge sharing. Similarly, an ideal M_2X_6 chain **2** is obtained from two ideal MX_4 chains via edge sharing. By repeating this process, one obtains an ideal MX_2 layer **3**. For our discussion, it is important to note that the layer **3** is also derived from the M_2X_6 chains **2** upon edge sharing. A projection view of **3** perpendicular to the layer is given by **4a**, which shows only the metal

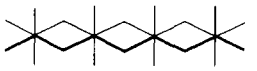

1

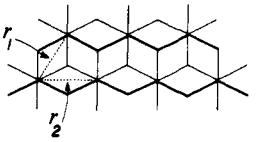

2

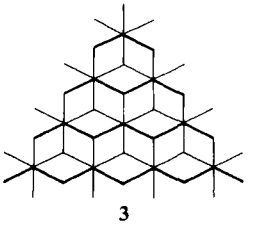

3

atoms and the upper triangle of X atoms around each metal. Ideal M_2X_6 chains have no metal–metal bonding as schematically

† The Laboratoire de Chimie Théorique is associated with the CNRS (UA 506) and belongs to ICMO and IPCM (Orsay).

(1) (a) Université de Paris-Sud. (b) Laboratoire de Chimie Théorique, Université de Rennes I. (c) Laboratoire de Chimie Minérale B, Université de Rennes I. (d) North Carolina State University.

(2) (a) Alcock, N. W.; Kjekshus, A. *Acta Chem. Scand.* **1965**, *19*, 79. (b) Wildervanck, J. C.; Jellinek, F. *J. Less-Common Met.* **1971**, *24*, 73.

(3) (a) van de Berg, J. M. *Inorg. Chim. Acta* **1968**, *2*, 216. (b) Anzenhofer, K.; de Boer, J. J. *Acta Crystallogr.* **1969**, *B25*, 1419. (c) Guillevic, J.; Le Marouille, J.-Y.; Grandjean, D. *Acta Crystallogr.* **1974**, *B30*, 111. (d) Chevrel, R.; Sergent, M.; Meury, J. L.; Quan, D. T.; Colin, Y. *J. Solid State Chem.* **1974**, *10*, 260. (e) Chevrel, R. Thèse d'Etat, Université de Rennes, 1974, pp 22–73. (f) Wada, H.; Onoda, M.; Nozaki, H.; Kawada, I. *J. Solid State Chem.* **1986**, *63*, 369.

0002-7863/89/1511-3778$01.50/0

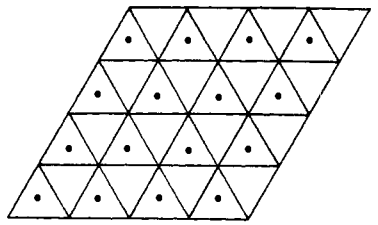

4a

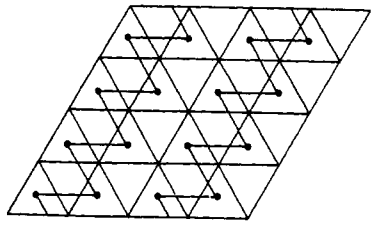

4b

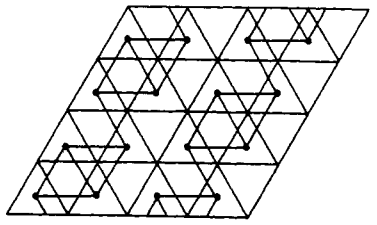

4c

represented by **5a**. Any real M_2X_6 chain of our interest is not ideal in shape due to the metal–metal bond formation across each shared octahedral edge between two MX_4 chains of the M_2X_6 chain. Thus, the M–M distance r_1 becomes short with respect to the M–M distance r_2 (see **2**). The M_2X_6 chain with such a distortion shows a metal clustering represented by **5b** (i.e., metal–metal zigzag chain).

5a

5b

5c

Description of the crystal structures containing MX_2 layers is simplified by adopting the following schemes: A perspective view of the ideal M_2X_6 chain is represented by **6**, in which only one

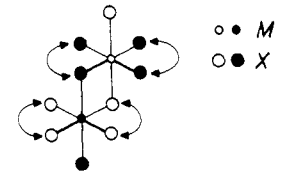

6

MX_6 octahedron is shown for each MX_4 chain for simplicity. We show the projection view of **6** along the chain direction by **7a**, in which two oxygen atoms indicated by a double-headed arrow in **6** are projected as one oxygen position. Then the corresponding view of the M_2X_6 chain with the metal-clustering **5b** is represented by **7b**, where the dashed line between the metal atoms signifies the short M–M distance.

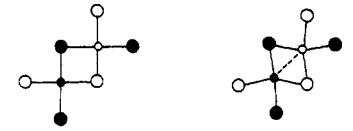

7a **7b**

An MX_2 layer having the metal-clustering **5b** is given by **4b**, which is simply derived from the M_2X_6 chains with the metal-clustering **5b** upon edge-sharing. Side-projection views of the MX_2 layers **4a** and **4b** can be given by **8a** and **8b**, respectively. In some cases, M_2X_6 chains with the metal-clustering **5b** undergo a further distortion to have the metal clustering shown in **5c**. An MX_2 layer with the metal-clustering **5c** is then given by **4c**.

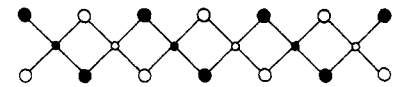

8a

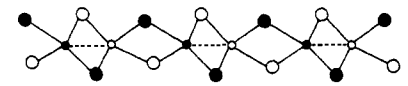

8b

Structural Patterns of MX_2 Layers

A. ReX_2 (X = S, Se).[2] This phase consists of ReX_2 layers, which are stacked together via van der Waals interactions. The metal atoms are in the oxidation state Re^{4+} (d^3) and the ReX_2 layers exhibit the metal-clustering **4c**.

B. $M'Mo_2S_4$ (M' = V, Cr, Fe, Co).[3] As shown in **9**, this phase

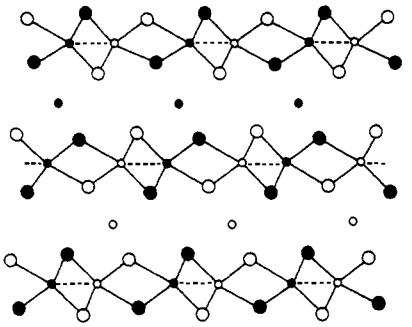

9

consists of MoS_2 layers. The M' atoms occupy the octahedral sites between the MoS_2 layers. One might consider **9** as a structure distorted from the so-called defect-NiAs structure[9] shown in **10**. A powder X-ray diffraction study of $CoMo_2S_4$ (with the space group $I2/m$)[3a] shows the metal-clustering **4b** in the MoS_2 layers

(4) (a) Bouchard, R. B.; Robinson, W. T.; Wold, A. *Inorg. Chem.* **1966**, *5*, 977. (b) Bouchard, R. B.; Wold, A. *J. Phys. Chem. Solids* **1966**, *27*, 591.

(5) (a) De Vries, A. B.; Jellinek, F. *Rev. Chim. Min.* **1974**, *11*, 624. (b) Kawada, I.; Nakano-Onoda, M.; Ishii, M.; Saeki, M.; Nakahira, M. *J. Solid State Chem.* **1975**, *15*, 246. (c) Kallel, A.; Boller, H. *J. Less-Common Met.* **1984**, *102*, 213. (d) Hold, S. L.; Bouchard, R. B.; Wold, A. *J. Phys. Chem. Solids* **1966**, *27*, 755.

(6) (a) de Jonge, R.; Popma, T. J. A.; Wiegers, G. A.; Jellinek, F. *J. Solid State Chem.* **1970**, *2*, 188. (b) Debliek, R.; Wiegers, G. A.; Bronsema, K. D.; van Dyck, D.; van Tendeloo, G.; van Landuyt, J.; Amelinckx, S. *Phys. Status Solidi A* **1983**, *77*, 249. (c) Debliek, R.; van Landuyt, J.; van Dyck, D.; van Tendeloo, G.; Amelinckx, S. *J. Solid State Chem.* **1987**, *70*, 108. (d) Hemmel, R.; van der Heide, H.; van Bruggen, C. F.; Haas, C.; Wiegers, G. In *Solid State Chemistry 1982, Proceedings of the 2nd European Conference*; Metselaar, R., Heijligers, H. J. M., Schoonman, R., Eds.; Elsevier: Amsterdam, 1983; p 691. (e) Rashid, M. H.; Sellmyer, D. J.; Katkanan, V.; Kirby, R. D. *Solid State Commun.* **1982**, *43*, 675. (f) Romanenko, A. I.; Rakhmenkulov, F. S.; Koropyatnik, I. N.; Fedorov, V. E.; Mischenko, A. V. *Phys. Status Solidi A* **1984**, *84*, K165. (g) Rastogi, A. K. *Phil. Mag. B* **1985**, *52*, 909.

(7) (a) Kadijk, F.; Huisman, R.; Jellinek, F. *Acta Crystallogr.* **1968**, *B24*, 1102. (b) Rashid, M. H.; Sellmyer, D. J. *Phys. Rev. B* **1984**, *29*, 2359.

(8) (a) Kertesz, M.; Hoffmann, R. *J. Am. Chem. Soc.* **1984**, *106*, 3453. (b) El Khalifa, M. A. Thèse de DEA, Universitē de Rennes, 1987. (c) For metal clustering in transition-metal oxides, see ref 18.

(9) Wells, A. F. *Structural Inorganic Chemistry*, 5th ed.; Clarendon: Oxford, 1984; p 167.

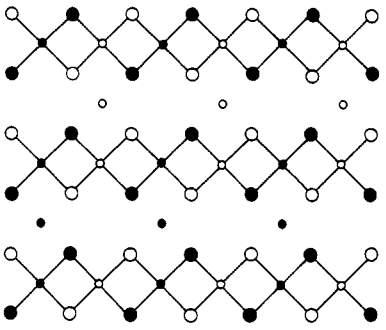

10

and so does a single-crsytal X-ray study (with the space group $C2/m$).[3b] However, a single-crystal X-ray study[3c] of $M'Mo_2S_4$ (M' = Fe, Co) with the space group Cc reveals the metal-clustering **4c**. Magnetic susceptibility measurements[3d-f] on $M'Mo_2S_4$ indicate the M' atoms to have the oxidation state +2, so that the MoS_2 layers consist of M^{3+} (d^3) ions. The $M'Mo_2S_4$ phase is semiconducting. The V_3X_4 (X = S, Se)[5] phase has a structure similar to **9** (i.e., $M'M_2X_4$ with M' = M = V). The VX_2 layers show the metal-clustering **4b**, and the V_3X_4 phase is metallic. The $M'Cr_2S_4$ (M' = Cr, V, Ni)[5d,10] phase has the structure **10**, and the CrS_2 layers do not show any metal clustering.

C. Mo_2S_3.[6] As depicted in **11**, the Mo_2S_3 phase is derived from

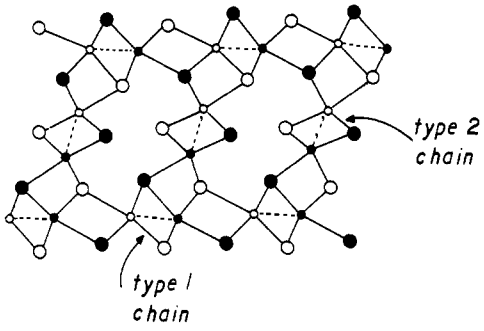

11

the $M'Mo_2S_4$ structure **9** by replacing each M' atom with an Mo_2S_2 unit, i.e., $(Mo_2S_2)Mo_2S_4 = (Mo_2S_3)_2$. This phase has Mo_2S_6 chains both in the MoS_2 layers (type 1) and between the layers (type 2).[6a-d] The two types of chains are nearly equivalent in that the Mo–Mo distances are about the same, and the Mo atoms have the oxidation state Mo^{3+} (d^3). Mo_2S_3 is metallic but undergoes charge density wave (CDW) transitions.[6] The type 1 and 2 chains have the metal-clustering **5b** before the CDW transitions but the metal-atom-clustering **5c** after the CDW transitions. M_2Se_3 (M = Nb, Ta)[7] has a structure similar to **11**, the type 1 and 2 chains of which have the metal-clustering **5b** and do not exhibit a CDW phenomenon.

Metal Clustering as a Peier's Distortion

Our survey in the previous section reveals that the metal-clustering **5c** in the M_2X_6 chains (equivalently, the metal-clustering **4c** in the MX_2 layers) occurs with d^3 metal ions and that the systems containing such chains either are semiconducting or exhibit a CDW phenomenon. With d^3 ions, the t_{2g} block bands of an M_2X_6 chain are half-filled. Thus the distortion **5b** → **5c** in an M_2X_6 chain, which doubles the unit cell size, would simply be a Peierls distortion[11] associated with the half-filled t_{2g} block bands. This is indeed the case, as we show by performing tight-binding band structure calculations[12] on representative examples with

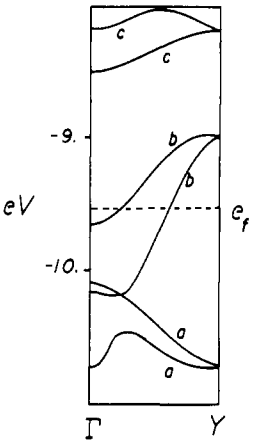

Figure 1. t_{2g} block bands of the Mo_2S_6 chain with the metal-clustering **5b**,[3a] where Γ = 0, $Y = b^*/2$, and the dashed line refers to the Fermi level.

Table I. Parameters and Exponents Used in the Calculations

atom	orbital	H_{ii} (eV)	ζ_1	ζ_2	c_1[a]	c_2[a]
S[16]	3s	−20.00	1.817			
	3p	−13.30	1.817			
Se[16]	4s	−20.50	2.44			
	4p	−13.20	2.07			
Nb[17]	5s	−10.10	1.90			
	5p	−6.86	1.85			
	4d	−12.10	4.08	1.64	0.6401	0.5516
Mo[17]	5s	−8.34	1.96			
	5p	−5.24	1.90			
	4d	−10.50	4.54	1.90	0.5899	0.5899

[a] Contraction coefficients used in the double-ζ expansion.

M_2X_6 chains. Our calculations are based upon the extended Hückel method,[13] and the atomic parameters employed in the present work are listed in Table I. In our discussion, we describe only the t_{2g} block bands since it is those bands that are partially filled and thus responsible for the electrical properties and potential structural instabilities.

A. M_2X_6 Chain and MX_2 Layer. Figure 1 shows the t_{2g} block bands calculated for the Mo_2S_6 chain with the metal-clustering **5b**, taken from the crystal structure of $CoMo_2S_4$ (space group $C2/m$).[3a] As described for the Nb_2S_6 chain of Nb_3S_4 elsewhere,[14] the flat bands a and c refer to metal–metal bonding and antibonding (across the shared edge between MX_4 chains), respectively. The band b is dispersive since it is composed of the x^2-y^2 orbitals pointed along the chain direction (see **12**). Figure 2 shows

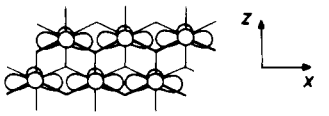

12

the t_{2g} block bands of the Mo_2S_6 chain with the metal-clustering **5c**, taken from the crystal structure of $CoMo_2S_4$ (space group Cc).[3b] With Mo^{3+} (d^3), the overall t_{2g} block bands are half-filled, so that the Mo_2S_6 chain with the metal-clustering **5b** does not have a band gap, but that with the metal-clustering **5c** does. Since the distortion **5b** → **5c** in the Mo_2S_6 chain of Mo^{3+} (d^3) ions doubles the unit cell size and also introduces a band gap, it is a Peierls distortion associated with the half-filled t_{2g} block bands.

Figure 3 shows the t_{2g} block bands of the MoS_2 layer **4b**, taken from the crystal structure of $CoMo_2S_4$ (space group $C_{2/m}$).[3a] Along the chain direction Γ → Y, the bands a, b, and c are very similar

(10) Jellinek, F. *Acta Crystallogr.* **1957**, *10*, 620.
(11) (a) Peierls, R. E. *Quantum Theory of Solids*; Oxford University Press: London, 1955; p 108. (b) Berlinsky, A. J. *Contemp. Phys.* **1976**, *17*, 331. (c) Whangbo, M.-H. *Acc. Chem. Res.* **1983**, *16*, 95. (d) Whangbo, M.-H. In *Crystal Structures and Properties of Materials with Quasi-One-Dimensional Sctructures*; Rouxel, J., Ed.; Reidel: Dordrecth, The Netherlands, 1986; p 27.
(12) Whangbo, M.-H.; Hoffmann, R. *J. Am. Chem. Soc.* **1978**, *100*, 6093.
(13) Hoffmann, R. *J. Chem. Phys.* **1963**, *39*, 1397. A modified Wolfsberg–Helmholz formula was used to calculate the off-diagonal H_{ij} values: Ammeter, J. H.; Bürgi, H.-B.; Thiebeault, J.; Hoffmann, R. *J. Am. Chem. Soc.* **1978**, *100*, 3686.
(14) Canadell, E.; Whangbo, M.-H. *Inorg. Chem.* **1986**, *25*, 1488.

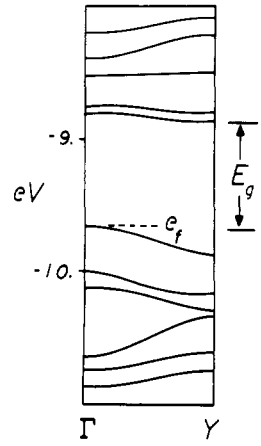

Figure 2. t_{2g} block bands of the Mo_2S_6 chain with the metal-clustering **5b**,[3b] where $\Gamma = 0$, $Y = b^*/2$, and E_g refers to the band gap.

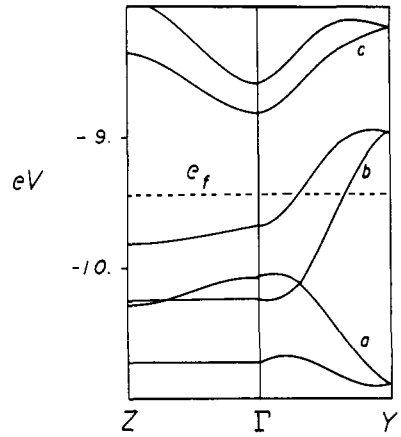

Figure 3. t_{2g} block bands of the MoS_2 layer with the metal-clustering **4b**,[3a] where $\Gamma = (0, 0)$, $Y = (0, b^*/2)$, and the dashed line refers to the Fermi level.

to those of the Mo_2S_6 chain shown in Figure 1. Along the interchain direction $\Gamma \rightarrow Z$, the bands a and b are nearly flat. Thus, as far as these two occupied bands are concerned, the Mo_2S_6 chains do not interact strongly in the MoS_2 layer. Figure 4 shows the t_{2g} block bands of the MoS_2 layer **4c**, taken from the crystal structure of $CoMo_2S_4$ (space group *Cc*).[3b] As expected by analogy with the Mo_2S_6 chains, the MoS_2 layer **4b** does not have a band gap, but the MoS_2 layer **4c** does.

It is clear from Figures 1–4 that the metal-clustering **4c** in the MX_2 layers of d^3 ions is a direct consequence of the Peierls distortion of its building blocks, M_2X_6 chains. The metal–metal distances found for the metal clusters of $CoMo_2S_4$[3c] and $ReSe_2$[2a] are shown in **13a** and **13b**, respectively. In both cases, the shortest

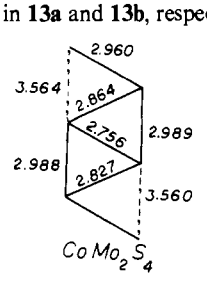

13a

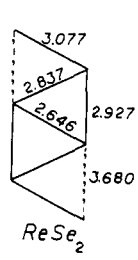

13b

metal–metal distance is the shorter diagonal distance of the "diamond" cluster. That is, the metal-clustering **5c** is a slight modification of the regular zigzag structure **5b**.

B. Metal Clustering and Electron Counting. According to the above discussion, MX_2 layers of d^3 ions are expected to undergo the metal-clustering **4c** and become semiconducting as a consequence. MX_2 layers of metal ions other than d^3 are not expected to show the metal clustering **4c** and hence remain metallic. With

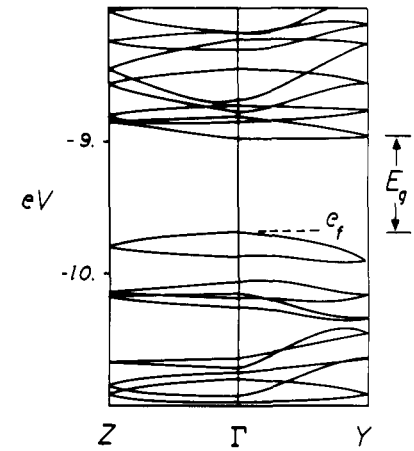

Figure 4. t_{2g} block bands of the MoS_2 layer with the metal-clustering **4c**,[3b] where $\Gamma = (0, 0)$, $Y = (0, b^*/2)$, and E_g refers to the band gap.

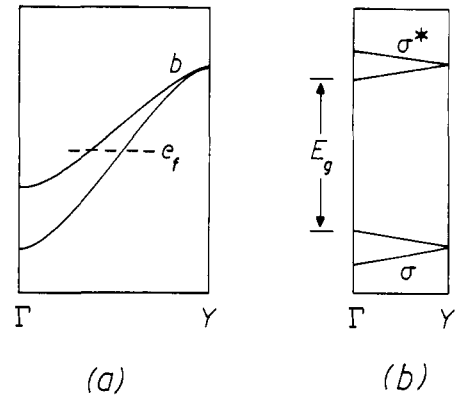

Figure 5. Schematic diagrams showing the essential change associated with the **5b** → **5c** distortion in the M_2X_6 chain: (a) the half-filled band a for the M_2X_6 chain with the metal-clustering **5b** and (b) the two split bands σ and σ^* for the M_2X_6 chain with the metal-clustering **5c**.

this generalization, we now comment on some $M'M_2X_4$ systems.

VMo_2S_4 is a semiconductor[3d-f] and is reported to have the metal-clustering **4b** in one study[3f] and **4c** in another study.[3e] Given the most likely oxidation state V^{2+} and hence the Mo^{3+} (d^3) ions in the MoS_2 layers, the crystal structure having the metal-clustering **4c** should be the correct structure. This is indeed the case.[3e,15]

NiV_2X_4 (X = S, Se)[4] is metallic and shows the metal-clustering **4b**. This suggests the oxidation state Ni^{2+} and hence the V^{3+} (d^2) ions in the VX_2 layers, which avoids the instability toward the metal-clustering **4c**. The V_3X_4 (X = S, Se)[5] phase (i.e., $M'M_2X_4$ with M' = M = V) is metallic and has the metal-clustering **4b** in the VX_2 layers. This is consistent with the oxidation states V^{2+} (d^3) and V^{3+} (d^2) in the M' and M sites, respectively. Our band structure calculations on V_3S_4 reveal that it is a multidimensional metal.

Neither the metal-clustering **4b** nor the metal-clustering **4c** is found in the CrS_2 layers of $M'Cr_2S_4$ (M' = Cr, V, Ni),[4b,10] despite the expected oxidation state Cr^{3+} (d^3) in the CrS_2 layers. If electron localization occurs in $M'Cr_2S_4$, as usual for many other Cr compounds, high-spin electron configurations would be appropriate for $M'Cr_2S_4$. Therefore the reasoning of the Peierls distortion based upon low-spin band filling does not apply.[11c,d] Nevertheless, Cr_3S_4 is a poor metal, which is possible if the partially filled e_g block bands of the M'^{2+} ions (i.e., Cr^{2+}) between

(15) X-ray oscillating Weissenberg photographs for a VMo_2S_4 single crystal clearly show a doubling of the monoclinic *b* axis (i.e., $b = 6.478$ A), which rules out the existence of a regular metallic zigzag chain: Chevrel, R., unpublished results.

(16) Canadell, E.; Whangbo, M.-H. *Inorg. Chem.* **1987**, *26*, 3974.
(17) Summerville, R. H.; Hoffmann, R. *J. Am. Chem. Soc.* **1976**, *98*, 7240.
(18) Burdett, J. K.; Hughbanks, T. *Inorg. Chem.* **1985**, *27*, 1741.

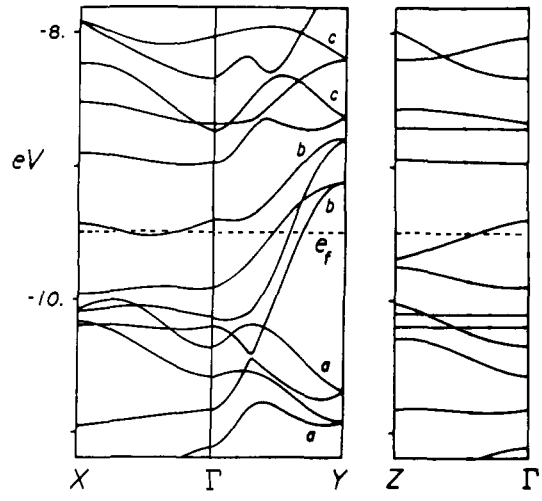

Figure 6. t_{2g} block bands of Mo_2S_3, where $\Gamma = (0, 0, 0)$, $X = (x^*/2, 0, 0)$, $Y = (0, b^*/2, 0)$, $Z = (0, 0, c^*/2)$, and the dashed line refers to the Fermi level.

the CrS_2 layers overlap with those of the M^{3+} ions (i.e., Cr^{3+}) in the CrS_2 layers.[5d]

The M′ atoms of $M'M_2X_4$ occupy the octahedral sites between the MX_2 layers. It is interesting to consider if the band gap of the MX_2 layer **4c** (Figure 4) would be closed up by possible interactions between the MX_2 layers via M′. Since the unit cell of $M'Mo_2X_4$ with the metal-clustering **4c** is large for band structure calculations, we examine this question qualitatively. The essential electronic structure change associated with the distortion **5b** → **5c** in the M_2X_6 chain is summarized in Figure 5, i.e., the half-filled band b is split into bands σ and σ^*. A unit cell of $M'M_2X_4$ has four M_2X_6 chains, so that eight σ and eight σ^* levels are present at Γ. These levels pair up along $\Gamma \rightarrow Y$ (e.g., Figure 5), but the crystal symmetry of $M'Mo_2X_4$ does not allow a pairing of σ levels with σ^* levels. Therefore, if the separation between the σ and σ^* levels is large in each M_2X_6 chain, the band gap of the MX_2 layer will not be closed up by interlayer interactions via M'^{2+} ions.

C. **Mo_2S_3 vs M_2Se_3 (M = Nb, Ta).** Mo_2S_3 has two CDW's, $k_1 = (0, b^*/2, 0)$ and $k_2 = (a^*/2, b^*/2, 0)$,[6b] which occur below 110 and 150 K, respectively. Mo_2S_3 is metallic after the two CDW transitions.[6d] This implies an imcomplete destruction of the Fermi surfaces by the CDW's and is possible when type 1 and 2 chains interact to some extent. Figure 6 shows the dispersion relations of the t_{2g} block bands calculated for the structure of Mo_2S_3 without the CDW modulations. Mo_2S_3 has one type 1 chain and one type 2 chain per unit cell. The six pairs of the t_{2g} block bands, clearly seen along the $\Gamma \rightarrow Y$ direction of Figure 6, are similar in nature to the t_{2g} block bands a, b, and c of Figure 1. The energy splitting in each of the bands a, b, and c suggests the presence of some interactions between type 1 and 2 chains and so do the dispersion relations along $\Gamma \rightarrow X$ and $\Gamma \rightarrow Z$ directions. The bands b, most dispersive along $\Gamma \rightarrow Y$ and partially filled, are likely to cause the CDW instabilities in Mo_2S_3. The absence of a permanent distortion in Mo_2S_3 (such as that found for $ReSe_2$ and $M'Mo_2S_4$) may be due to the interactions between type 1 and 2 chains. For example, a permanent distortion in type 1 chains may cause severe strain on type 2 chains and vice versa.

M_2Se_3 (M = Nb, Ta)[7] has a structure similar to **9**, as does Mo_2S_3. The metal-clustering **5b** is found for type 1 and 2 chains,

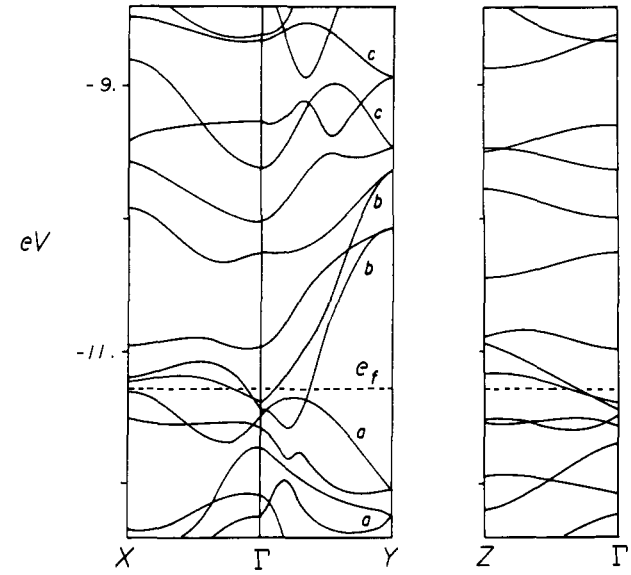

Figure 7. t_{2g} block bands of Nb_2Se_3, where $\Gamma = (0, 0, 0)$, $X = (a^*/2, 0, 0)$, $Y = (0, b^*/2, 0)$, $Z = (0, 0, c^*/2)$, and the dashed line refers to the Fermi level.

but the two types of chains are not equivalent in that the M–M bond is longer in type 2 chains. Unlike Mo_2S_3, M_2Se_3 does not show a CDW phenomenon, which reflects the fact that the M_2Se_6 chains contain d^2 ions instead of d^3 ions. Figure 7 shows the t_{2g} block bands calculated for Nb_2Se_3, which have the feature similar to those of Figure 6. The bottom portion of the dispersive bands b overlaps with the bands a. With d^2 ions, the Fermi level of M_2Se_3 cuts the region in which the bands are dispersive in all directions, $\Gamma \rightarrow X$, $\Gamma \rightarrow Y$, and $\Gamma \rightarrow Z$ (see Figure 7). Therefore, M_2Se_3 (M = Nb, Ta) is a metal and does not show a CDW phenomenon.

Concluding Remarks

Except for systems such as $M'Cr_2S_4$ (M′ = V, Cr, Ni) in which electron localization is presumably important, our study leads to the following conclusions: MX_2 layers of d^2 ions show the metal-clustering **4b** (or equivalently, the metal-clustering **5b**, in its M_2X_6 chains). This is caused by the metal–metal bond formation in the M_2X_6 chain across each shared octahedral edge between MX_4 chains. MX_2 layers of d^3 ions show the metal-clustering **4c** (or equivalently, the metal-clustering **5c**, in its M_2X_6 chains). This is a consequence of the Peierls distortion associated with the half-filled t_{2g} block bands of individual M_2X_6 chains. Therefore, the MX_2 layers of d^3 ions cannot be semiconducting without the metal-clustering **4c**. Mo_2S_3 consists of two types of M_2X_6 chains, i.e., those in the MX_2 layers and those between the MX_2 layers. Mo_2S_3 has Mo^{3+} (d^3) ions and shows metal clustering not as a permanent distortion but as a CDW. This is due to some interactions between the Mo_2S_3 layers via the intervening Mo_2S_6 chains. M_2Se_3 (M = Nb, Ta) contains M_2Se_6 chains with d^2 ions and consequently shows the metal-clustering **4b** and metallic behavior.

Acknowledgment. This work was supported by NATO, Scientific Affairs Division, and also by DOE, Office of Basic Sciences, Division of Materials Science, under Grant DE-FG05-86ER45259.

Registry No. $CoMo_2S_4$, 12356-95-5; V_3S_4, 12138-16-8; Mo_2S_3, 12033-33-9; Nb_2Se_3, 12266-23-8.